Composites: Part B 45 (2013) 1384–1390

Contents lists available at SciVerse ScienceDirect

Composites: Part B

journal homepage: www.elsevier.com/locate/compositesb

Dual effectiveness of freezing–thawing and sulfate attack on high-volume slag-incorporated ECC

Erdoğan Özbay [a,*], Okan Karahan [b], Mohamed Lachemi [c], Khandaker M.A. Hossain [c], Cengiz Duran Atis [b,d]

[a] Civil Eng. Department, Mustafa Kemal University, Iskenderun, Hatay, Turkey
[b] Civil Eng. Department, Erciyes University, Kayseri, Turkey
[c] Civil Eng. Department, Ryerson University, Toronto, Ontario, Canada
[d] Civil Eng. Department, Abdullah Gul University, Kayseri, Turkey

ARTICLE INFO

Article history:
Received 5 May 2012
Received in revised form 29 June 2012
Accepted 8 July 2012
Available online 17 August 2012

Keywords:
A. Fibers
B. Cure behavior
B. Environmental degradation
D. Mechanical testing

ABSTRACT

This study investigated the dual effect of freeze–thaw cycles with sodium sulfate solution on the performance of non-air-entrained Engineering Cementitious Composites (ECCs) with high volumes of slag. ECC specimens containing three different levels of slag content as a replacement for cement (55%, 69% and 81% by weight of total cementitious material) were exposed to aggressive sodium sulfate solution under freezing–thawing cycles. The load–deflection response associated with ultimate mid-span deflection and flexural strength/stiffness was determined, along with crack development behavior. For comparison purposes, the freezing–thawing resistance (in water) of control ECC specimens was also evaluated. Modified point count method air-void parameters, compressive strength, porosity, water absorption and sorptivity tests were also conducted on the virgin ECC specimens (those not exposed to freezing–thawing cycles in water or aggressive sodium sulfate solution). The test results for the virgin specimens revealed that increased slag content (S/PC) improved the ductility, hardened air content, water absorption, porosity and sorptivity of ECC, while marginally decreasing the compressive and flexural strengths. Freeze–thaw cycles in water or sodium sulfate solution showed that the ductility of ECC specimens decreased remarkably, irrespective of slag content and applied freezing–thawing process. Reduction in mass loss was at minimal levels and no significant behavior change was monitored between the specimens undergoing freeze–thaw cycling in water and the aggressive sodium sulfate solution. Moreover, the decrease in flexural stiffness was more evident than the reduction of the flexural strength for all ECC mixtures.

1. Introduction

The durability of cement-based composites is based on degrees of resistance to frost, corrosion, permeation, carbonation, chemical attack such as sulfate attack. Generally, properties of cement-based composites are measured under the single action of one of the deterioration mechanisms mentioned above [1–5]. However, in real field exposure, damage to cement-based composite structures often occurs due to multiple mechanisms acting in a combined and possibly synergistic manner. Therefore, it is vital to develop performance tests that mobilize multiple damage mechanisms to improve our understanding of their combined effects on emerging concretes and cement-based composites [6]. Although limited data is currently available on the long-term performance of elements/structures made of normal, high-strength and self-compacting concretes under multiple damaging mechanisms, no research has been done to date on the dual effects of freeze–thaw (F–T) cycling with sodium sulfate solution on the properties of Engineered Cementitious Composites (ECCs).

ECC is a special type of high-performance fiber-reinforced cementitious composite designed with micromechanical principles [7–15]. Micromechanical design allows for optimization of the composite for high performance, resulting in extreme tensile strain capacity while minimizing the amount of reinforcing fibers (typically less than 2% by volume). The materials used in the production of standard ECC mixtures are Portland cement, Class-F fly ash, micro-silica sand, water, polyvinyl alcohol fiber, and a polycarboxylic-ether type high range water reducing admixture (HRWR) [16]. Unlike ordinary cement-based materials, ECC strain-hardens after first cracking, much like a ductile metal, and demonstrates a strain capacity 300–500 times greater than normal concrete [17]. This unique tensile strain-hardening behavior results from an elaborate design using a micromechanics model that takes the interactions among fiber, matrix and fiber–matrix interface into account [18]. ECC can significantly enhance the durability of structures exposed to aggressive environments, such as F–T cycles, hot water immersion, chloride immersion, deicing-salt exposure and

* Corresponding author.
E-mail address: ozbay@mku.edu.tr (E. Özbay).

1359-8368/$ - see front matter Crown Copyright © 2012 Published by Elsevier Ltd. All rights reserved.
http://dx.doi.org/10.1016/j.compositesb.2012.07.038

alkali-silicate reaction. These properties, along with the relative ease of production including self-consolidation casting and shotcreting, make ECC materials suitable for various civil engineering applications such as high-rise buildings, bridges, tunnels, highways, and other forms of infrastructure [19,20].

In this research study, ECC mixtures were produced and evaluated using slag (S) instead of fly ash; slag is a by-product of pig iron manufacturing. Partial replacement of slag, like fly ash, reduces the environmental burden. Substituting slag for Portland cement up to 70% improved the flexural deflection and the tensile strain capacities of ECC. The addition of slag can also enhance durability; for instance, it provides better sulfate and chloride ion penetration resistance. It also results in a more homogeneous fiber distribution because slag particles provide a driving force for fiber dispersion [21].

As mentioned earlier, ECCs are suitable for tunnels, highways, and other forms of infrastructure. Recently, the usage of ECC has increased in the construction of these types of structures, which are often concomitantly exposed to sulfate rich environments and frost action [22]. To evaluate the resistance of high-volume slag-incorporated ECC mixtures to the dual effect of freezing–thawing cycles and aggressive sulfate attack, this study produced non-air-entrained high-volume slag-incorporated ECCs and accelerated testing procedures for ECC specimens, combining their exposure to aggressive sodium sulfate solution with freezing–thawing cycles. The results were compared with those of the control specimens subjected to freezing–thawing cycles with water, which are commonly used as the sole performance measure of the quality of cement-based composites under frost action [23].

2. Experimental studies

2.1. Materials and mixture proportions

Type I general use Portland cement (PC) and ground granulated blast furnace slag (S) with a Blaine specific surface area of 430 m^2/kg were used in all three ECC mixtures developed for this study. The hydraulic activity index of slag was category 80, according to ASTM C 989 [24]. Physical properties and chemical compositions of the PC and slag are listed in Table 1. All ECC mixtures included micro-silica sand with a maximum grain size of 250 μm and a mean size of 110 μm, and a polycarboxylic-ether type high range water reducing admixture (HRWR) with a solid content of approximately 30%. The polyvinyl alcohol (PVA) fiber used had a length of 8 mm, a diameter of 39 μm, tensile strength of 1600 MPa and density of 1300 kg/m^3. The fiber surface is coated with 1.2% oil by weight to reduce the fiber–matrix chemical and friction bond [25]. In all ECC mixtures, the fiber content was kept constant at 2% by volume. All produced high-volume slag-incorporated ECC contained no air-entraining admixture.

Table 1
Characteristics of Portland cement and slag.

Chemical analysis	Cement	Slag
SiO_2	21.72	38.4
Al_2O_3	5.96	10.64
Fe_2O_3	3.6	0.79
CaO	60.78	34.2
MgO	2.64	6.94
K_2O	0.75	0.84
Na_2O	0.17	0.16
SO_3	2.17	1.48
P_2O_5	0.04	0.07
TiO_2	0.36	0.71
Cr_2O_3	0.0455	0.01
Mn_2O_3	0.1496	1.84
LoI	2.0	3.09
$SiO_2 + Al_2O_3 + Fe_2O_3$	31.28	49.83
Physical properties		
Blaine (m^2/kg)	350	430
45 μm	4.5	1
Density	3.18	2.87

Details of the three high-volume slag-incorporated ECC mixtures with S/PC of 1.2, 2.2 and 4.2 by weight are provided in Table 2. Mixtures were prepared in a standard mortar mixer with a constant amount of cementitious materials and a constant water (W) to cementitious material (CM) ratio (W/CM) of 0.27, and a micro-silica sand (SS) to cementitious material ratio (SS/CM) of 0.36. HRWR was added to the mixture until the desired fresh ECC characteristics were visually observed. The amount of HRWR admixture in each mixture was adjusted to achieve consistent rheological properties for better fiber distribution and workability. All three ECCs therefore have similar fresh properties with self-consolidating performance [26]. As seen in Table 2, increasing the S/PC ratio from 1.2 to 4.2 slightly decreased the HRWR needed to reach the desired consistent fresh ECC characteristics. It is well known that ground granulated blast furnace slag is a latent hydraulic material and when incorporated with PC, its reaction must be initiated by calcium hydroxide released from hydration. Therefore, slag retards the hydration of blended cement and prolongs setting time. Also, fine slag particles fill the spaces among the cement particles and improve particle size distribution [27]. Most probably, for the combined above-mentioned aspects, the need for HRWR decreased with the increase in slag content [28].

2.2. Mixing, specimens and curing

A Hobart mixer was used in preparing all ECC mixtures. Solid ingredients, including Portland cement, slag and aggregate, were first mixed at 100 rpm for 1 min. Water and HRWR admixture were added into the dry mixture and mixed at 150 rpm for another minute, then at 300 rpm for 2 min to produce a consistent ECC matrix. A liquefied fresh mortar matrix should reach a consistent and uniform state before adding fibers; after examining it to ensure there was no clumping at the bottom of the mixer, PVA fiber was added and mixed at 150 rpm until all fibers were evenly distributed [26].

Several $400 \times 100 \times 75$ mm and $355 \times 50 \times 75$ mm prism specimens were cast from each mixture and subjected to freezing–thawing tests and determination of air-void characteristics, respectively. The compressive strength of ECC mixtures was computed as an average of six 50-mm cube specimens. Water absorption, porosity and sorptivity tests were also performed on at least three companion 50-mm virgin cube specimens at the age of 28 days. All specimens were cast in one layer without any compaction and demolded at the age of 24 h. Compressive strength, water absorption, porosity and sorptivity specimens were cured in sealed plastic bags at 95 ± 5% RH, 23 ± 2 °C for 7 days. The specimens were then air cured at 50 ± 5% RH, 23 ± 2 °C until the age of 28 days. Hardened air void and frost resistance specimens were subjected to moist curing in lime-saturated water at 23 ± 2 °C for 13 days. Fourteen days after

Table 2
Mix properties of high-volume slag-incorporated ECC mixtures.

Ingredients	S/PC = 1.2	S/PC = 2.2	S/PC = 4.2
Water (W) (kg/m^3)	380	379	378
Cement (PC) (kg/m^3)	576	395	242
Slag (S) (kg/m^3)	691	868	1017
Silica sand (SS) (kg/m^3)	456	455	454
Fiber (PVA) (kg/m^3)	26	26	26
HRWRA (kg/m^3)	5.4	5.2	4.5
S (%)	55	69	81
S/PC	1.2	2.2	4.2
SS/CM	0.36	0.36	0.36
W/CM	0.30	0.30	0.30
Strength 28 days (MPa)	61.7	59.2	56.1

casting, the beam specimens were moved into the freeze–thaw chamber in accordance with ASTM C666 Procedure A [29].

Several specimens were subjected to a 5% (by mass) sodium sulfate solution and the remaining specimens were placed in normal tap water. All of the specimens were subjected to 300 cycles, which included five to six freezing and thawing cycles in a 24-h period. Change in mass loss was measured every 30 cycles, and both the sodium sulfate solution and tap water were renewed. The load–deflection response, mid-span deflection, flexural strength, flexural stiffness and residual crack width of the specimens were determined by testing four replicate specimens under four-point loading before freezing and thawing cycles. Similarly, after exposure to 300 freezing–thawing cycles in sodium sulfate solution or tap water, a four-point bending test was performed under displacement control at a loading rate of 0.005 mm/s on a closed-loop controlled servo-hydraulic material test system with a span length of 360 mm and a height of 75 mm to determine residual flexural performance and bending load–deflection curves. For each high-volume slag-incorporated ECC mixture, four companion freeze–thaw specimens were tested.

The air-void parameters of the high-volume slag-incorporated ECC mixtures on polished specimens were determined by a modified point count method according to ASTM C457 [30]. Measurements were made on the hardened ECC using a microscope, and the air void parameter was examined by scanning along a series of traverse lines. Air content, spacing factor (maximum distance from any point in the cement paste to an air-void boundary) and specific surface (ratio of the surface area of the air voids to their volume) were used to characterize the air voids [31]. In general, a good quality, frost-resistant concrete requires a spacing factor of less than 0.20 mm and a specific surface greater than 25 mm^{-1}.

3. Results and discussions

3.1. Air void analysis

It is generally recognized that the air void structure of cement-based composites is a critical parameter for durability, especially when subjected to freezing–thawing action [31]. The basic characteristics of the air void analysis of the hardened non-air-entrained high-volume slag-incorporated ECC are presented in Table 3. In the three non-air-entrained ECC mixtures, the specific surface fluctuated between 18.3 and 23.2 mm^{-1} and the spacing factor between 0.28 mm and 0.37 mm. These spacing factor values were somewhat higher than the suggested limits for producing durable concrete to withstand severe cold weather [32,33]. However, it must be kept in mind that high-volume slag-incorporated ECCs are produced without deliberate air entrainment. As seen in Table 3, although no deliberate air-entrainment was added to the slag-incorporated ECC mixtures, the hardened-air contents of these mixtures had values of 7.5%, 7.1% and 6.6% for the ECC mixtures with S/PC ratios of 1.2, 2.2 and 4.2, respectively. ACI committee 345 [34] recommended air content ratios for bridge deck concretes subjected to freezing, mentioning that the air content of any mixture depends on aggregate gradation, fine aggregate content, slump, concrete temperature and mixing time. Their recommended air content volume varied based on aggregate size; the lower the aggregate size, the higher the recommended air content value. For the 9.5 mm nominal maximum aggregate size, the recommended air content value was 7.5%. As mentioned earlier, the maximum grain size of the micro-silica sand used in the slag-incorporated ECC was 250 μm, which means that the above-mentioned hardened air-content seemed to be adequate in terms of freeze–thaw durability. As also seen in Table 3, an increase in S/PC from 1.2 to 4.2 decreased the air content and spacing factors significantly, while augmenting the specific surface only slightly. Most probably, the relatively fine slag particles (Blaine fineness 430 m^2/kg, see Table 1) could have filled the space, resulting in denser microstructure of the ECC [35]. Generally, a higher slag content in an ECC mixture lowers the hardened air content and spacing factor.

Table 3
Air-void characteristics of ECC mixtures.

Properties	S/PC = 1.2	S/PC = 2.2	S/PC = 4.2
Air content (%)	7.5	7.1	6.6
Specific surface (mm^{-1})	18.3	20.7	23.2
Spacing factor (mm)	0.37	0.29	0.28

3.2. Compressive strength

The compressive strength test results of the high-volume slag-incorporated ECC mixtures at 28 days are listed in Table 2. Six 50-mm compression cubes were used to define the average compressive strengths according to ASTM C39 [36] procedures. The compressive strength of ECC decreased marginally with the increase of S/PC or slag content (from 55% to 81%); however, even at 81% replacement of Portland cement with slag (S/PC = 4.2), the compressive strength at 28 days was about 55 MPa. A reduction in compressive strength at early ages of up to 28 days was observed due to the pozzolanic activity of minerals that may only be effective in the long term; ECC produced with a high volume of slag requires a longer period of moist curing [37].

3.3. Flexural strength

The flexural strength, mid-span deflection capacity at peak stress, and residual crack width of 14-day moist-cured high-volume slag-incorporated ECC samples (tested before exposure to freezing–thawing cycles) are presented in Table 4. Fig. 1 also shows the representative 14-day flexural strength/mid span deflection response curves of high-volume slag-incorporated ECCs. As can be seen in both Table 4 and Fig. 1, an increase in S/PC improved the ductility (deformation capacity) of ECC significantly. This result can be attributed to the lower matrix toughness and the improved fiber–matrix interface due to increased slag content [21]. As demonstrated

Table 4
Flexural properties of high-volume slag-incorporated ECC mixtures according to applied environmental condition.

Applied condition	Mixture ID	Mid-span deflection (mm)	Flexural strength (MPa)	Relative stiffness (%)	Residual crack width (μm)
14 days moist cured and tested before F–T cycles	S/PC = 1.2	2.63	11.85	100	72
	S/PC = 2.2	3.99	11.72	100	69
	S/PC = 4.2	4.16	10.18	100	63
After 300 F–T cycles in water	S/PC = 1.2	1.44	10.21	65	130
	S/PC = 2.2	1.47	9.78	70	120
	S/PC = 4.2	1.89	8.98	68	119
After 300 F–T cycles in sulfate solution	S/PC = 1.2	1.55	10.25	69	126
	S/PC = 2.2	1.57	9.93	74	123
	S/PC = 4.2	1.88	9.07	78	116

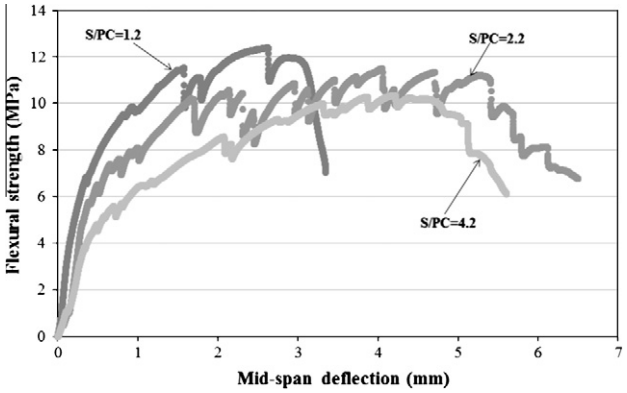

Fig. 1. Flexural strength-mid span deflection curve of high-volume slag-incorporated virgin ECC mixtures (before exposure to freeze–thaw cycles).

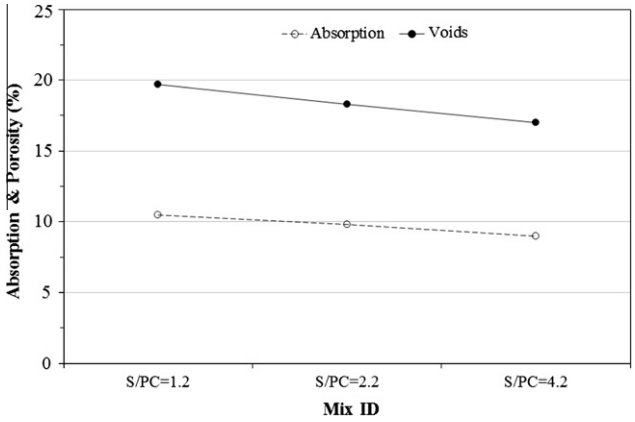

Fig. 3. Water absorption and porosity test results of high-volume slag-incorporated virgin ECC mixtures.

in Fig. 2, under the four-point bending load, the high-volume slag-incorporated ECC prisms containing 55–81% slag underwent plastic deformation similar to a metal plate. Based on the flexural strength-mid span deflection curve of the ECC mixtures in Fig. 1, it can be concluded that all slag-incorporated ECC mixtures exhibited strain hardening behavior, and mid-span deflection value at peak load reached 4.16 mm with total displacement at more than 6.5 mm for the S/PC = 4.2 mixture. On the other hand, the increase in slag content only marginally influenced flexural strength, and at 81% replacement of Portland cement with slag (S/PC = 4.2), flexural strength was more than 10.0 MPa. An increase in S/PC from 1.2 to 4.2 only decreased the flexural strength values from 11.85 to 10.18 MPa.

Table 4 also presents the effects of slag content on residual crack width. All tested specimens were inspected under a microscope to measure crack width. All crack width measurements were conducted in the unloaded stage, and widths were measured on the tension surface of the prism specimens along the span length of 120 mm. It was observed that residual crack width decreased slightly as S/PC or slag content increased. Increased slag content led to a smaller residual crack width. As shown in Table 1, slag has a higher Blaine fineness value than Portland cement, which means it contains a higher number of small particles. More small particles result in better packing at the fiber–matrix interface and improved interfacial property. As a result, crack widths may get smaller with increased slag content [21]. Development of multiple tight micro-cracks (less than 80 μm) instead of one crack with large crack width is the foremost property of ECC (see Fig. 2).

3.4. Water absorption, porosity and sorptivity

Fig. 3 presents the results of water absorption and porosity tests. It shows that increasing the S/PC ratio from 1.2 to 4.2 gradually decreased both water absorption and porosity. For instance, the ECC mixture with an S/PC of 4.2 had 9.0% and 17.0% water absorption and porosity values, respectively, compared to 10.5% and 19.7% for ECC with an S/PC of 1.2. The slight reduction in water absorption and porosity reflected a finer pore structure that would, for example, inhibit ingress of aggressive elements into the pore system [38]. Increasing slag content from 55% to 81% resulted in a decrease in the total volume of air in hardened ECC and in a corruption of the air void system exhibited by a decrease of micropore content. The decreased water absorption and porosity of ECC mixtures were proportional to the decreased spacing of the air voids and hardened air content.

The change in absorption (mm) with time ($s^{0.5}$) depended on the S/PC of ECC mixtures, as demonstrated in Fig. 4. This test was chosen as it measures the rate of ingress of water through unsaturated ECC specimens. The results of cumulative water absorption per unit area in the 50-mm cube specimen up to 6 h was used for linear regressions, and the slope of the regression equation was used to describe the sorptivity of ECC mixtures. It is clear from Fig. 4 that the rate of water absorption increased systematically with an increase in testing time, and that there was a significant reduction in the sorptivity coefficient of ECC mixtures. For instance, increasing the S/PC from 1.2 to 2.2 and from 2.2 to 4.2

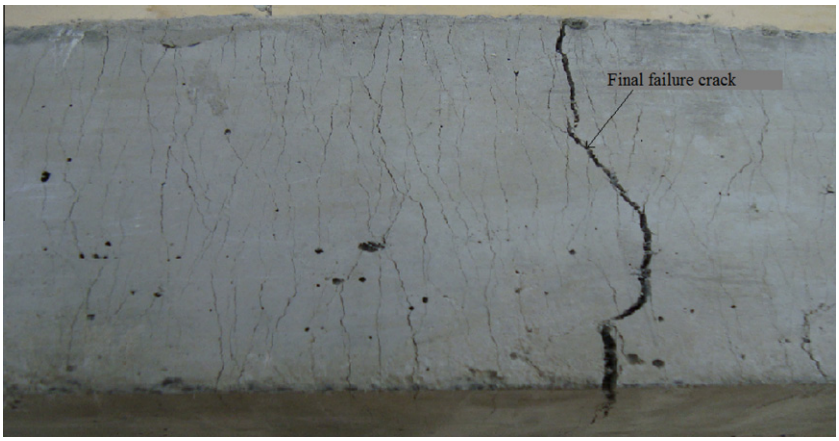

Fig. 2. Typical cracking patterns of ECC prism specimens after flexure load applications (S/PC = 4.2).

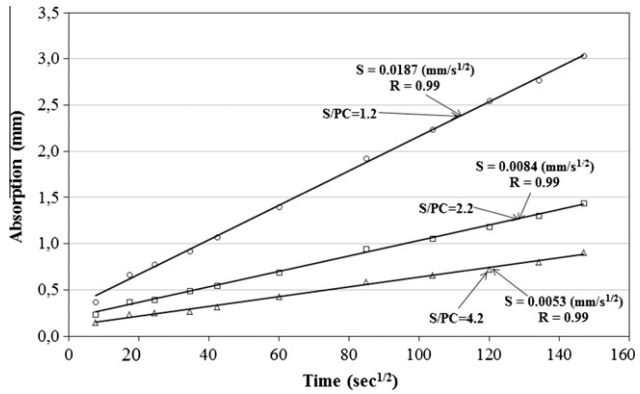

Fig. 4. Sorptivity results of high-volume slag-incorporated virgin ECC mixtures.

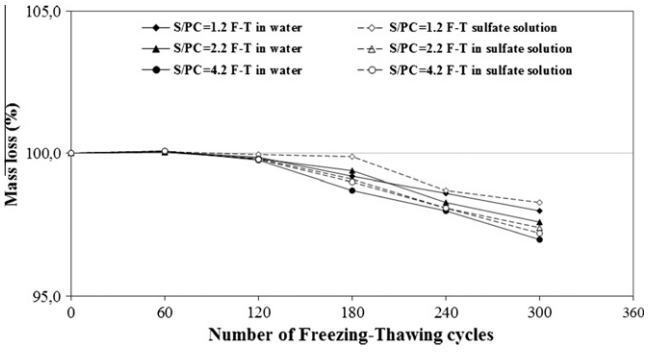

Fig. 5. Mass loss changes of ECC mixtures depending on the number of freezing and thawing cycles.

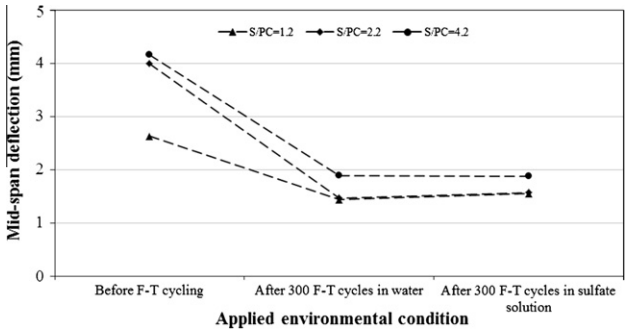

Fig. 6. Mid-span deflection variation of ECC mixtures according to applied environmental condition.

decreased the sorptivity coefficient from 0.0187 to 0.0084 mm/s$^{0.5}$ and from 0.0084 to 0.0053 mm/s$^{0.5}$, respectively (see Fig. 4, slope of line). The rate of reduction was around 55% and 36%, respectively. As seen in Fig. 4, the correlation coefficient (r) between the absorption (mm) and testing time (s$^{0.5}$) was very high (0.99) for all the high-volume slag-incorporated ECC mixtures.

3.5. Freezing–thawing cycling in water or sodium sulfate solution

After 300 F–T cycles in water (reference) or in sodium sulfate solution, visual inspection of all non-air-entrained high-volume slag-incorporated ECC specimens showed no change or only slightly visible damage. Deterioration of specimens during F–T cycles was evaluated by computing mass loss, flexural strength, mid-span deflection, relative stiffness and residual crack width variations. Fig. 5 presents the variation of mass loss according to the applied freezing–thawing process (in water or in sodium sulfate solution), S/PC and number of F–T cycles. As per Fig. 5, the mass of the specimens increased slightly up to 60 F–T cycles; however, it was generally less than 0.1%, with a maximum mass gain of 0.08% for the S/PC = 4.2 ECC mixture in water. The reason behind the mass gain was most probably the absorption of water or sodium sulfate solution and the formation of reaction products in the voids [39]. Beyond 60 F–T cycles, a slight decrease was monitored in the mass of specimens; at the end of 300 F–T cycles, maximum mass loss was approximately 3.0% for the S/PC = 4.2 ECC mixture in water. A marginal increase was observed in the mass loss of ECC mixtures depending on the applied freezing–thawing process and S/PC. Generally, an increase in S/PC increased mass loss. The experimental results showed that the mass loss of ECC subjected to F–T cycles in sodium sulfate solution was fractionally lower than that in water, as shown in Fig. 5. According to Miao et al. [1], this result may be related to the differences in physical

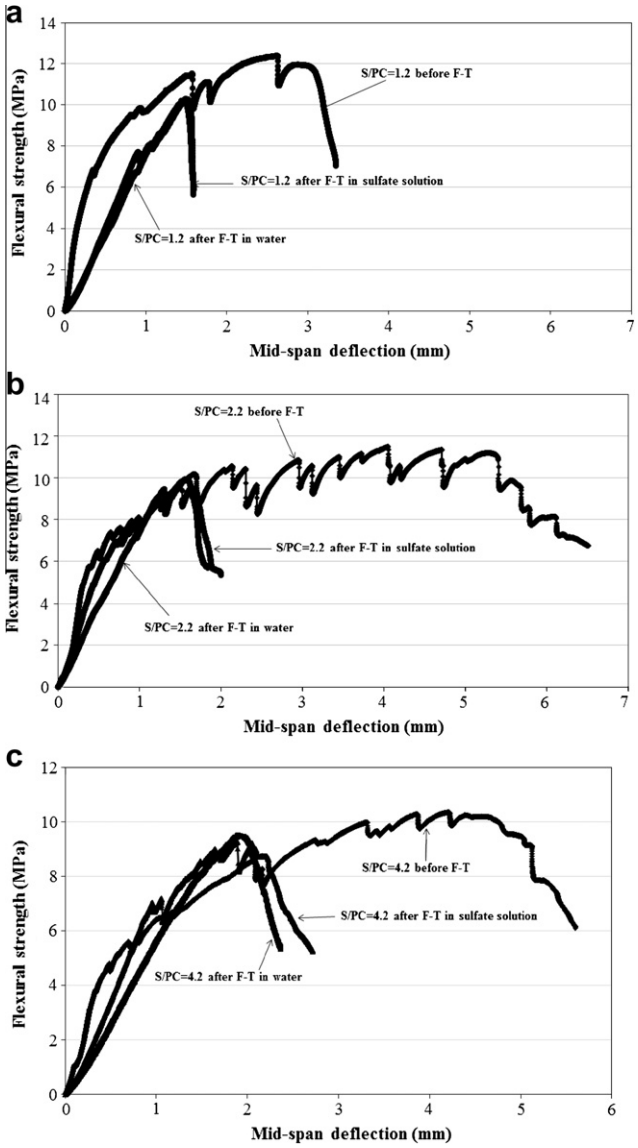

Fig. 7. Variation of flexural strength-mid span deflection values of ECC mixtures after exposure to freezing and thawing cycle: (a) S/PC = 1.2; (b) S/PC = 2.2; (c) S/PC = 4.2.

properties of frozen water and solution, such as freezing point, deformability or ductility. Normally, in the classical form of sulfate attack, sodium sulfate (Na_2SO_4) reacts with portlandite (CH), monosulfate and unreacted C_3A to form gypsum ($C\bar{S}H_2$) and ettringite ($C_6A\bar{S}_3H_{32}$), which can cause expansion, cracking, and deterioration of concrete [6]. However, 2 months of F–T cycles in sulfate solution may not be enough to form gypsum or ettringite. Very little scaling was observed on the surface of high-volume slag-incorporated ECC prisms, irrespective of S/PC and applied freezing–thawing process.

Table 4 and Figs. 6 and 7 present the variation in mid-span deflection of ECC mixtures. Ductility of the ECC mixtures (represented by mid-span deflection) decreased remarkably, regardless of S/PC and applied freezing–thawing process. As seen in both figures, no significant difference was observed on the average mid-span deflection value of ECC specimens subjected to F–T cycles in water or sodium sulfate solution. For instance, the average mid-span deflection values of S/PC = 2.2 ECC mixture were 3.99, 1.47 and 1.57 mm before F–T cycles, after 300 F–T cycles in water and after 300 F–T cycles in sulfate solution, respectively. These results contradict previous research [19]. Sahmaran et al. [19] assessed the durability of non-air-entrained fly-ash-incorporated ECC under F–T cycles. They concluded that 55% fly-ash-incorporated ECC without air entrainment showed excellent resistance to freezing and thawing, with minimal reduction in ductility. They also mentioned that increases in pore volume greater than approximately 0.30 μm in diameter and intrinsically high tensile ductility due to the presence of micropolyvinyl alcohol fibers could be the reasons behind a lower reduction in ductility. However, although the same polyvinyl alcohol fiber was used in this research, the ductility of high-volume slag-incorporated ECC mixtures decreased along with the effect of frost action. Despite a notable reduction in ductility, after undergoing 300 F–T cycles in water or sodium sulfate solution, high-volume slag-incorporated ECC specimens retained a mid-span deflection capacity more than a hundred times that of normal concrete with no environmental exposure [19].

The main parameters that control resistance to freezing and thawing are air content and spacing factor [40]. According to the air void analysis results in Table 3, the ECC mixtures with the lowest air void spacing factor (0.28 mm) were severely deteriorated during freezing and thawing in water or sulfate solution; average mid-span deflection decreased from 4.16 mm to about 1.88 mm. An increase in slag content most probably led to a finer pore structure. However, large pores (generally larger than 0.3 μm in diameter) were beneficial to frost resistance of concrete, whereas small and intermediate-size pores were detrimental to the frost resistance of cement-based composites [19].

Table 4 and Fig. 7 illustrate the flexural strength variations for the high-volume slag-incorporated ECC prism specimens before and after exposure to 300 F–T cycles in water or sodium sulfate solution. The decreased flexural strength of ECC mixtures due to freezing and thawing, which is most probably due to the formation of microcracks, was found to be similarly influenced by the applied freezing–thawing process. Both of the applied freezing–thawing processes (in water or in sodium sulfate solution) moderately degraded the flexural strength; the reduction rate for ECC mixtures was around the same level. For instance, flexural strengths of ECC mixtures with 55% slag were 11.85, 10.21 and 10.25 MPa before F–T cycles, after 300 F–T cycles in water and after 300 F–T cycles in sulfate solution, respectively. The lowest flexural strength was observed in the S/PC = 4.2 ECC mixture after 300 F–T cycles in water. Fig. 8 presents the relative stiffness and flexural strength fluctuations of ECC mixtures. It demonstrates that an increase in slag content slightly augmented the deterioration of flexural strength. The slope of the flexural stress/mid span deflection curve represents the stiffness of the ECC prisms. Fig. 8 shows that the

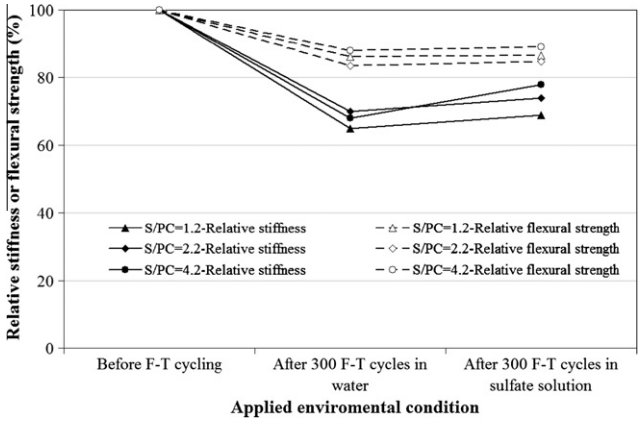

Fig. 8. Variation of relative stiffness and flexural strength according to applied environmental condition.

slope or stiffness decreases when ECC specimens are subjected to F–T cycles. It can be noted from Fig. 8 that the reduction in stiffness is significantly higher than the reduction in flexural strength. Like flexural strength, the stiffness loss of the ECC specimens subjected to F–T cycles in sodium sulfate solution was marginally lower than those subjected to freeze–thaw in water. The sodium sulfate solution had both positive and negative effects on the high-volume slag-incorporated ECC mixtures when subjected to F–T cycles; the positive effect was that when ECC specimens were immersed in solution, sodium sulfate permeated into the pores and the concentration of pore solution increased, which led to a drop in its freezing point. This drop was beneficial in that it reduced damage in specimens more effectively than in those subjected to F–T cycles in water [1]. The negative effect was concrete degradation resulting from the sulfate attack. In the present case, as seen in Table 4 and Figs. 5–8, the positive effect of sodium sulfate solution was dominant, showing slightly less degradation than the fresh water specimens.

Table 4 also shows the residual crack width of the high-volume slag-incorporated ECCs after being subjected to freeze–thaw action. The residual crack width of all ECC mixtures at ultimate flexural load was less than 130 μm. As mentioned in previous research [41], for crack widths of less than about 135 μm, the effect of crack on effective chloride diffusion and mass loss of steel reinforcement was marginal when compared with the virgin specimens. Among the three high-volume slag-incorporated ECCs, the mixture with the S/PC of 4.2 showed the smallest residual crack width regardless of the applied environmental condition. Residual crack width in the specimens subjected to F–T cycles in water was higher than for those in the sodium sulfate solution. After exposure to F–T cycles in water or sodium sulfate solution, residual crack width widened considerably, with a rate of increment of around 85%. Pigeon et al. [40] hypothesized that the tensile stresses due to freezing in frost-susceptible systems will always be higher than the tensile strength at some point, and thus cracks will always be formed. As a result of flexural loading, cracks occurring due to F–T cycles got wider.

4. Conclusions

The following conclusions have been drawn from the study:

- All high-volume slag-incorporated ECC virgin beam specimens (those not subjected to F–T cycles) exhibited multiple cracking and strain hardening behavior under four-point bending. Increasing the amount of slag in ECC led to an increase in ductility

(measured in terms of peak deflection) and also to a remarkable decrease in residual crack width. All ECC mixtures showed average mid-span deflection values higher than 2.65 mm and residual crack widths smaller than 80 μm.

- For the virgin ECC specimens, despite a marginal reduction in compressive and flexural strength with increased slag content, significant improvements were observed in water absorption, porosity, sorptivity and hardened air-void parameters.
- After 300 freeze–thaw cycles in sodium sulfate solution or water, ECC specimens were found to be quite similarly influenced. ECC mixtures exhibited somewhat less degradation when freezing and thawing was conducted in 5.0% sodium sulfate solution rather than in water.
- After 300 freeze–thaw cycles, a significant reduction was monitored in the mid-span deflection behavior (a measure of ductility) of ECC beam specimens, regardless of slag content and applied environmental process. The highest mid-span deflection reduction was observed at the highest slag replacement level, where average mid-span deflection was decreased from 4.16 mm to 1.88 mm.
- The rate of decrease in flexural strength and mass was much lower than that observed in mid-span deflection under freeze–thaw cycles. At the end of 300 freeze–thaw cycles in water, maximum flexural strength and mass loss were around 17% and 3.0%, respectively, for ECC mixtures with an S/PC of 4.2.
- In ECC beam specimens subjected to freeze–thaw cycles, the decrease in relative stiffness was much more evident than that observed in relative flexural strength. After 300 freeze–thaw cycles in water, the drop in relative stiffness was around 35% compared to a 17% drop in relative flexural strength for ECC mixtures with an S/PC of 4.2.
- Despite exposure to 300 freeze–thaw cycles, whether in sodium sulfate solution or in water, residual crack width of all ECC mixtures at ultimate flexural load was smaller than 130 μm. Residual crack widths of specimens subjected to freeze–thaw cycles in sodium sulfate solution were slightly larger.

Acknowledgments

The authors gratefully acknowledge the financial assistance of The Council of Higher Education of Turkey (YOK), the Natural Sciences and Engineering Research Council (NSERC) of Canada, and the Canada Research Chair Program.

References

[1] Miao C, Mu R, Tian Q, Sun W. Effect of sulfate solution on the frost resistance of concrete with and without steel fiber reinforcement. Cem Concr Res 2002;32:31–4.
[2] Zhou Y, Cohen MD, Dolch WL. Effect of external loads on the frost resistant properties of mortar with and without silica fume. ACI Mater J 1994;91:595–601.
[3] Schneider U, Nagele E. Stress corrosion of cement mortars in ammonium sulfate solution. Cem Concr Res 1993;23:13–9.
[4] Zivica V, Szabo V. The behaviour of cement composite under compression load at sulfate attack. Cem Concr Res 1994;24:1475–82.
[5] Schneider U, Nagele E, Dumat F. Stress corrosion induced cracking of concrete. Cem Concr Res 1986;16:535–44.
[6] Bassuoni MT, Nehdi ML. Durability of self-consolidating concrete to sulfate attack under combined cyclic environments and flexural loading. Cem Concr Res 2009;39:206–26.
[7] Li VC. ECC-tailored composites through micromechanical modeling, fiber reinforced concrete: present and the future. In: Banthia N, et al., editors. CSCE, Montreal, QC, Canada; 1998. p. 64–97.
[8] Li VC. On engineered cementitious composites (ECCs) – a review of the material and its applications. Adv Concr Technol 2003;1:215–30.
[9] Li VC, Wang S, Wu C. Tensile strain-hardening behavior of PVA–ECC. ACI Mater J 2001;98:483–92.
[10] Sahmaran M, Li VC. De-icing salt scaling resistance of mechanically loaded engineered cementitious composites. Cem Concr Res 2007;7:1035–46.
[11] Sahmaran M, Li VC, Li M. Transport properties of engineered cementitious composites under chloride exposure. ACI Mater J 2007;104:604–11.
[12] Sahmaran M, Li VC. Durability of mechanically loaded engineered cementitious composites under high alkaline environment. Cem Concr Comps 2008;30:72–81.
[13] Sahmaran M, Li VC, Andrade C. Corrosion resistance performance of steel-reinforced engineered cementitious composite beams. ACI Mater J 2008;105:243–250.
[14] Sahmaran M, Li VC. Influence of microcracking on water absorption and sorptivity of ECC. Mater Struct 2009;42:593–603.
[15] Li M, Sahmaran M, Li VC. Effect of cracking and healing on durability of engineered cementitious composites under marine environment, high performance fiber reinforced cement composites (HPFRCC-5) Stuttgart. Germany 2007;10–13:313–22.
[16] Sahmaran M, Lachemi M, Hossain KMA, Li VC. Internal curing of engineered cementitious composites for prevention of early age autogenous shrinkage cracking. Cem Concr Res 2009;39:893–901.
[17] Sahmaran M, Lachemi M, Hossain KMA, Ranade R, Li VC. Influence of aggregate type and size on ductility and mechanical properties of engineered cementitious composites. ACI Mater J 2009;106:308–16.
[18] Li VC, Leung CKY. Theory of steady state and multiple cracking of random discontinuous fiber reinforced brittle matrix composites. J Eng Mech 1992;118:2246–64.
[19] Sahmaran M, Lachemi M, Li VC. Assessing the durability of engineered cementitious composites under freezing and thawing cycles. J ASTM Int 2009;6:1–13.
[20] Sahmaran M, Lachemi M, Li VC. Assessing mechanical properties and microstructure of fire-damaged engineered cementitious composites. ACI Mater J 2010;107:297–304.
[21] Zhou J, Qian S, Beltran MGS, Ye G, van Breugel K, Li VC. Development of engineered cementitious composites with limestone powder and blast furnace slag. Mater Struct 2010;43:803–14.
[22] http://ace-mrl.engin.umich.edu//NewFiles/eccapp.html.
[23] Bassuoni MT, Sonebi M. Effect of freezing thawing cycles on the resistance of self-consolidating concrete to sulfate attack, design, production and placement of self-consolidating concrete, RILEM book series 1. Springer; 2010. p. 329–40.
[24] ASTM C989/C989M-11. Standard specification for slag cement for use in concrete and mortars, ASTM vol. 04.02. West Conshohocken, PA; 2003.
[25] Li VC, Wu C, Wang S, Ogawa A, Saito T. Interface tailoring for strain-hardening PVA–ECC. ACI Mater J 2002;99:463–72.
[26] Yang EH, Yang Y, Li VC. Use of high volumes of fly ash to improve ECC mechanical properties and material greenness. ACI Mater J 2007;104:620–8.
[27] Li Z, Ding Z. Property improvement of Portland cement by incorporating with metakaolin and slag. Cem Concr Res 2003;33:579–84.
[28] Palacios M, Puertas F, Alonso MM, Bowen P, Houst YF. Compatibility of PC superplasticizers with slag-blended cements. In: Holland TC, Gupta P, Malhotra VM, editors. Ninth ACI international conference on superplasticizers and other chemical admixtures, Seville, Spain; 2009.
[29] ASTM C666/C666M-03. Standard test method for resistance of concrete to rapid freezing and thawing, ASTM vol. 04.02. West Conshohocken, PA; 2008.
[30] ASTM C457/C457M-11. Standard test method for microscopical determination of parameters of the air void system in hardened concrete, ASTM vol. 04.02. West Conshohocken, PA.
[31] Elsen J. Automated air void analysis on hardened concrete: results of a European inter comparison testing program. Cem Concr Res 2001;31:1027–31.
[32] Powers TC. Topics in concrete technology 3: mixtures containing intentionally entrained air. J PCA Dev Lab 1964;6:19–42.
[33] Powers TC. Topics in concrete technology 3: characteristics of air-void systems. J PCA Dev Lab 1965;7:23–41.
[34] ACI committee 345, proposed revision of ACI 345-74: standard practice for concrete highway bridge deck construction. Concr Int 1981;3:19–53.
[35] Wu X, Jiang W, Roy DM. Early activation and properties of slag cement. Cem Concr Res 1990;20:961–74.
[36] ASTM C39/C39M-12 standard test method for compressive strength of cylindrical concrete specimens, ASTM vol. 04.02. West Conshohocken, PA.
[37] Demirboga R, Turkmen I, Karakoc MB. Relationship between ultrasonic velocity and compressive strength for high-volume mineral-admixtures concrete. Cem Concr Res 2004;34:2329–36.
[38] Khatip JM, Hibbert JJ. Selected engineering properties of concrete incorporating slag and metakaolin. Constr Build Mater 2005;19:460–72.
[39] Duchesne J, Bérubét MA. Effect of supplementary cementing materials on the composition of cement hydration products. Adv Cem-Base Mater 1995;2:42–53.
[40] Pigeon M, Azzabi M, Pleau R. Can microfibers prevent frost damage? Cem Concr Res 1996;26:1163–70.
[41] Sahmaran M, Yaman IO. Influence of transverse crack width on reinforcement corrosion initiation and propagation in mortar beams. Can J Civ Eng 2008;35:236–245.